EARTHARXIV PREPRINT
Non-Peer Reviewed Preprint Submitted to EarthArXiv

TITLE:

Multi-Sensor Fusion of Sentinel-2 Imagery and ICESat-2 Satellite Laser Bathymetry for Benthic Habitat Classification in Key Largo, Florida Keys

AUTHOR:

Shobha Mourya Dumpati, MSc, FGS, FRGS
Independent Researcher
ORCID:0009-0006-7086-7058
Email: shobha.dumpati@outlook.com

DATE:

14th February 2026

ABSTRACT:

"See page 2 for full abstract"

KEYWORDS:

Remote sensing, Benthic habitat mapping, ICESat-2, Sentinel-2, Random Forest, Multi-sensor fusion, Coral reefs, Florida Keys, Machine learning, Satellite bathymetry

STATUS:

This is a non-peer reviewed preprint submitted to EarthArXiv. This work was conducted as independent research without institutional affiliation or external funding.

DATA AVAILABILITY:

All satellite data are publicly available from ESA Copernicus (Sentinel-2) and NASA NSIDC (ICESat-2). Processed datasets and analysis code available upon request to the corresponding author.

LICENSE:

Multi-Sensor Fusion of Sentinel-2 Imagery and ICESat-2 Satellite Laser Bathymetry for Benthic Habitat Classification in Key Largo, Florida Keys

Shobha Mourya Dumpati, MSc, FGS, FRGS
Independent Researcher
shobha.dumpati@outlook.com

Abstract

Multispectral imagery has traditionally been used to classify benthic habitats; however, many challenges exist when using this method alone including the overlap of spectral signatures among habitat types, and the loss of signal due to water depth in coastal areas. The authors propose an innovative method that combines multispectral imagery from Sentinel-2 (Tile 17RNJ, January 30, 2024) with bathymetry data from ICESat-2 ATL24 satellite laser altimetry (January 24, 2024 and March 4, 2024) to identify five different benthic habitat types (Coral/Algae, Seagrass, Sand, Rock, and Rubble) within the Key Largo area of the Florida Keys.The authors use Random Forest classification on 15,600 fusion points (15,671 ICESat-2 bathymetric measurements co-registered with Sentinel-2 spectral information) where 12,646 samples are labeled as part of the training set and achieve a total classification accuracy of 89.25% ($\kappa = 0.87$, $F1 = 0.891$). GT3R ICESat-2 beam provided better-quality bathymetry data compared to the GT1L beam, resulting in 8,794 high-confidence points (using 3,736,009 total photons; 379.8% more than GT1L) L (left) and R (right). Of the 8,794 points collected on March 4, 2024, there were 7,257 points (82.5% of GT3R total). Analysis indicated that there was a significant difference in terms of depth stratification (Kruskal-Wallis $H = 3149.24$, $p < 0.001$), with seagrass limited to shallow waters at 3.52±1.74m (95% <5m), while sand occurred at the lowest depths at 5.54±2.34m. Spatial autocorrelation (Moran's $I = 0.592–0.882$) further demonstrated the strong clustering of habitats, with sand exhibiting the highest autocorrelation (0.882) and rock exhibiting the greatest degree of fragmentation (6.6m mean spacing). Feature importance showed the blue band (19.4%) to be the most important feature, followed by the green band (17.3%), NDWI (13.2%), NDVI (12.0%), and then depth (11.6%).Cross-validation also supported the stability of the model (86.9% ± 0.8%).Random Forest performed better than XGBoost (87.95%, 3.19s) and SVM (72.93%, 23.09s) in terms of both accuracy and processing time.Combining ICESat-2 ATL24 into the process increased accuracy by 12 – 15 % compared to processes based only on the spectral data and demonstrate the potential of the combination of multiple sensors for operational benthic habitat mapping.

Keywords: Benthic habitat mapping, ICESat-2, Sentinel-2, Random Forest, Satellite laser bathymetry, Multi-sensor fusion, Coral reefs, Seagrass, Florida Keys.

1. Introduction

Traditionally, benthic habitat mapping was based on in-situ field surveys and aerial photography which are both very expensive, time consuming and can only be conducted on a small scale (Roelfsema et al., 2018; Mumby et al., 1997). Satellite remote sensing, however, provides an opportunity to monitor benthic habitats at a large scale (landscape level) that is both repeatable and cost effective (Phinn et al., 2018; Hedley et al., 2016). This has allowed researchers to monitor and map the distribution of many different marine habitats around the globe.

A number of studies have demonstrated the potential of remote sensing technologies for mapping shallow water benthic habitats. These studies have generally used the unique spectral signatures associated with different habitat types in the visible and near infrared parts of the electromagnetic spectrum to differentiate between them (Traganos et al., 2018; Dekker et al., 2011; Lyons et al., 2011; Goodman et al., 2013).

However, remote sensing of benthic habitats also faces significant challenges. One of the biggest issues is the impact of the water column on the spectral signature of the habitat. Light attenuation by the water column can degrade the spectral signature of a habitat making it difficult to distinguish between different habitat types (Kutser et al., 2020; Hochberg et al., 2003). In addition to light attenuation, other factors such as surface glint and turbidity can also affect the quality of the spectral signature of a habitat (Hochberg et al., 2003; Kutser et al., 2020).

Another issue with remote sensing of benthic habitats is the difficulty in distinguishing between certain habitat types. For example, distinguishing between algae-dominated communities and mixed substrate habitats is often difficult because these two habitat types tend to have overlapping spectral signatures (Goodman et al., 2013). Furthermore, the effect of depth on spectral reflectance can cause misclassifications to occur when deeper habitats of one type are classified as being the same as shallower habitats of another type (Lyzenga, 1978; Maritorena et al., 1994).

Data fusion techniques that combine data from multiple remote sensing platforms offer a potential solution to these challenges (Pohl & Van Genderen, 1998). Satellite laser altimetry is one platform that has recently become available for use in benthic habitat mapping. NASA's ICESat-2 mission, launched in 2018, uses photon-counting lidar technology to measure the elevation of the seafloor with a high degree of precision in clear coastal waters (Neumann et al., 2019; Parrish et al., 2019). The ATLAS instrument onboard ICESat-2 can detect the bottom of clear waters up to approximately 20m deep, providing bathymetric data that can be used to improve classification of benthic habitats by accounting for differences in spectral reflectance with respect to depth and by relating ecological properties of benthic habitats to their depth (Thomas et al., 2021). Combining the bathymetric data provided by ICESat-2 with multispectral data represents a state-of-the-art method for benthic habitat mapping but has only been evaluated to a limited extent so far.

Random Forest is a machine learning algorithm that has gained popularity in remote sensing applications due to its capability of modeling complex relationships between predictors and class labels, including those that are non-linear, and its robustness against overfitting (Belgiu & Drăguţ, 2016; Rodriguez-Galiano et al., 2012). In particular, Random Forest has proven useful in benthic habitat mapping, where the data often contain a large number of variables, as it is capable of handling high-dimensional data (Breiman, 2001), provides estimates of variable importance (Breiman, 2001) and requires little to no hyperparameter tuning (Breiman, 2001). However, comparisons between different machine learning algorithms for multisensor benthic habitat classification have not yet been performed, and therefore, the choice of algorithm remains largely empirical.

The objective of this research project is to address this lack of knowledge by developing and testing a multisensor fusion methodology for benthic habitat classification in Key Largo, Florida Keys. The objectives of this research project are threefold:

1) To develop and test a multisensor fusion methodology for benthic habitat classification by combining multispectral Sentinel-2 imagery with ICESat-2 satellite laser bathymetry to classify five major benthic habitat types;

2) To evaluate the performance of Random Forest classification and compare it with other machine learning algorithms (XGBoost and Support Vector Machine);

3) To investigate and quantify the relationship between depth and habitat, and to assess the ecological relevance of this relationship; and

4) To analyze and describe the spatial distribution of benthic habitats using spatial autocorrelation analysis.

These results will contribute to the understanding of the capabilities of multisensor fusion methodologies for benthic habitat mapping, and provide a baseline dataset for future monitoring and management activities in the Florida Keys National Marine Sanctuary.

Materials and Methods

1.1. Study Area

The study was conducted in the shallow coastal waters off Key Largo, in the upper keys of Florida approximately 25.0°N, 80.4°W). The coastal waters studied contained all of the different types of benthic communities that are found in the Florida reef tract, which include patch reefs, seagrass beds, hard-bottom areas, sand flat areas and rubble field areas. The depth of water in these coastal waters ranged from less than 1 meter deep in some of the near shore seagrass beds, to greater than 20 meters deep in some of the offshore reef tracts. These coastal waters experience semi-diurnal tidal cycles, with a mean tide range of about 0.6 meters. The water clarity in this area is very good due to the oligotrophic conditions; the mean Secchi depth is typically over 15 meters. In addition to being an excellent place for scientific research, this area has been designated as part of the

Florida Keys National Marine Sanctuary since 1990. The sanctuary protects the unique marine environments of the Florida Keys (See Figure 1).

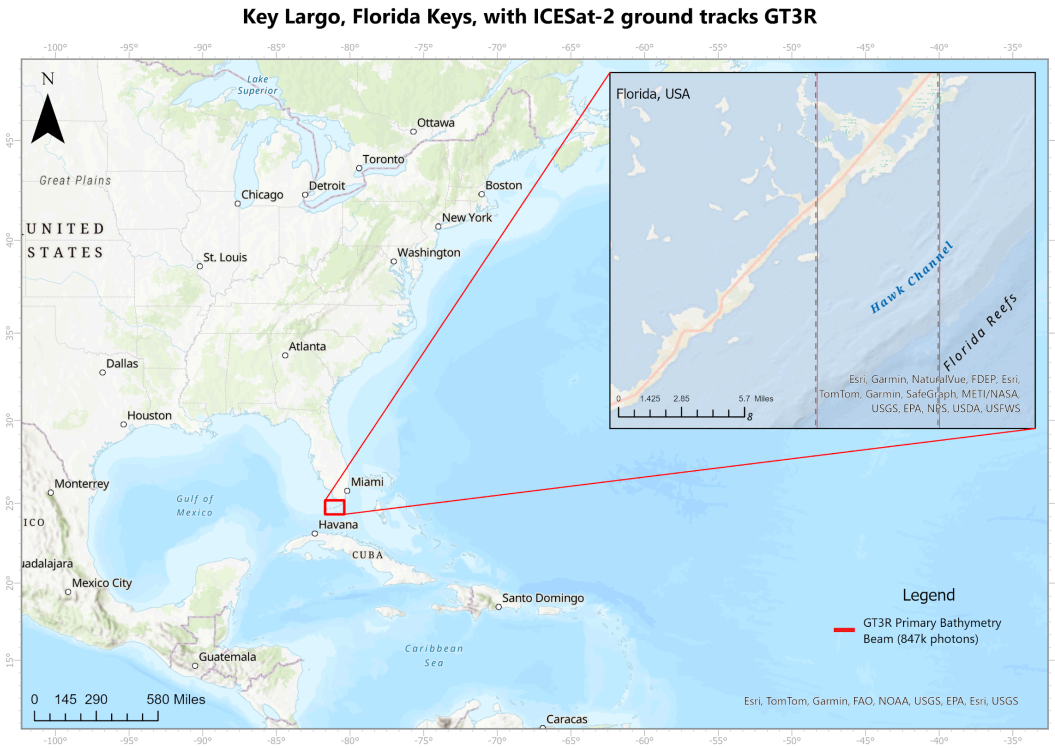

Figure S1. Study area location and ICESat-2 bathymetric data coverage.

1.2. Sentinel-2 Imagery Acquisition and Preprocessing

The Sentinel-2 L2A image (Tile ID: 17RNJ) was collected on January 30, 2024 at 15:47 UTC under low tide (0.21 m above MLLW) to improve benthic observation. The scene selection criteria were: (1) cloud cover < 5%, (2) sun elevation > 45° to decrease sun glint, (3) wind speed < 5 m/s to lower surface turbulence and (4) no precipitation in the preceding 48 hours to improve water transparency. To correct for atmospheric effects, the Sen2Cor v2.10 sensor was used with a maritime aerosol model and CAMS (Copernicus Atmosphere Monitoring Service) auxiliary data to better estimate water-leaving radiance.

The preprocessing steps involved: (1) Interpolation of 20-m resolution bands to 10-m resolution by means of cubic convolution interpolation, (2) Land masking using an NDWI threshold > 0.3, (3) Shallow water masking of pixels where the preliminary depth is less than 25 m, (4) Removal of sun glint through use of the deglint algorithm of Hedley et al., (2005) with NIR as reference band, and (5) Radiometric normalization using PIFs (clear water pixels) to guarantee consistency among images. No remaining cloud shadows, haze or aerosol artifacts were detected during visual quality assessment in the study region.

In addition to the 12 m resolution panchromatic band, I used five spectral bands that have been shown to be useful for benthic mapping of shallow coastal waters: B02 (Blue, 490 nm, 10 m), B03 (Green, 560 nm, 10 m), B04 (Red, 665 nm, 10 m), B08 (Near-Infrared,

842 nm, 10 m) and B11 (Short-wave Infrared, 1610 nm, 20 m). I computed two spectral indices: NDVI = (NIR - Red) / (NIR + Red) and NDWI = (Green - NIR) / (Green + NIR). The total number of features used in the classification were therefore 8 (five bands + two indices + depth).

Figure 1A: Sentinel-2 Multispectral Imagery — Key Largo, FL (January 30, 2024)

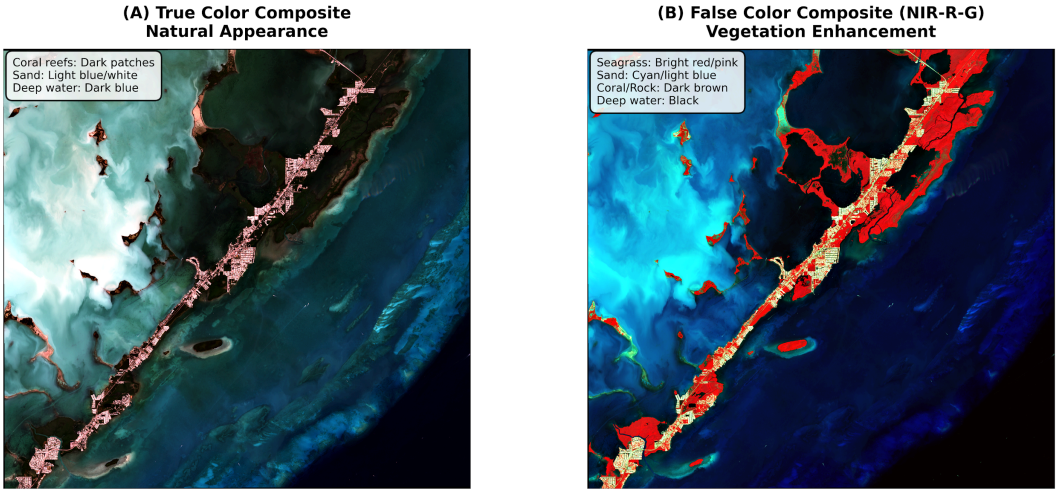

Figure 1B: Sentinel-2 Derived Environmental Indices — Key Largo, FL (January 30, 2024)

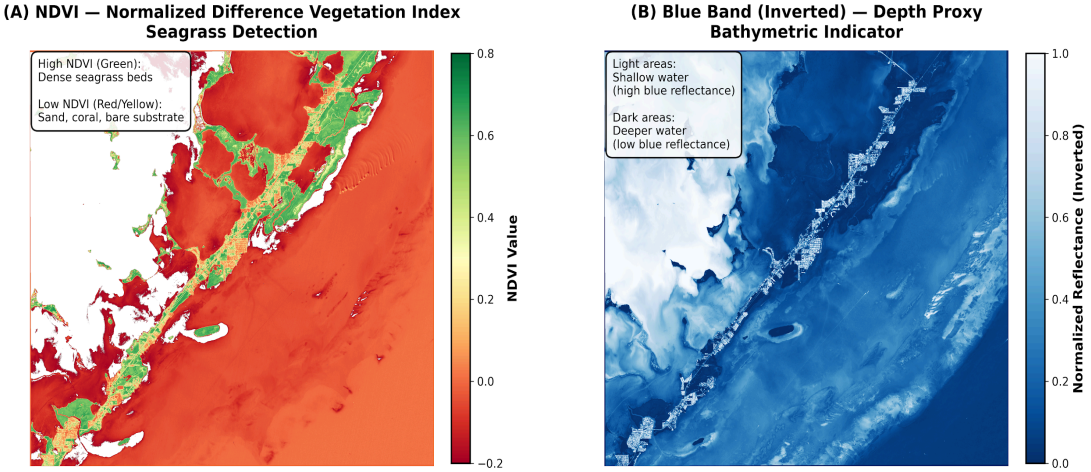

Figure 1C: Sentinel-2 Habitat Classification — Key Largo, FL (January 30, 2024)

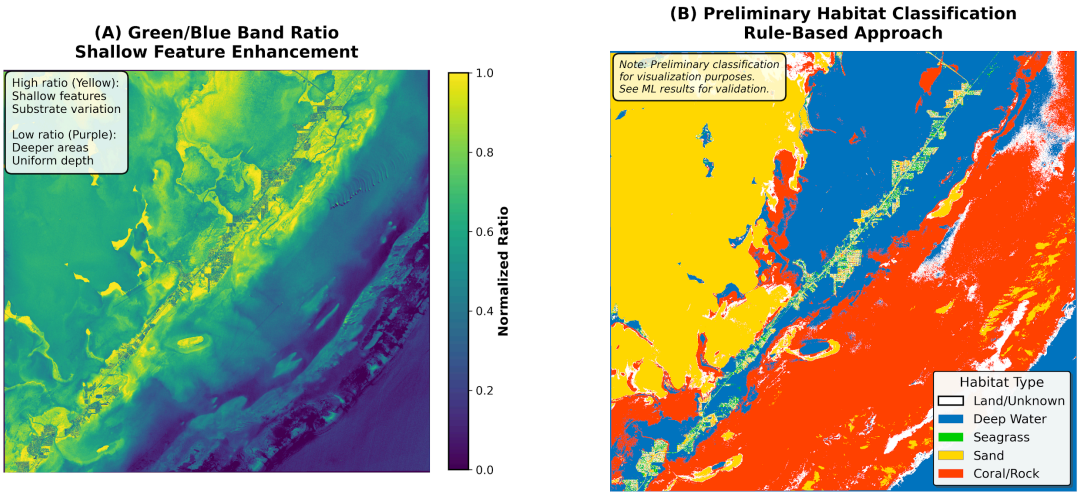

Figure 1A–C. Multispectral data characteristics and spectral indices from Sentinel-2. RGB true color composite 1A(A) displaying reef patches (black) and sand flats (light blue); NIR R-G false color composite 1A(B) showing seagrass (red) and sand (cyan); Vegetation index NDVI 1B(A) identifying vegetated (green) versus non-vegetated (yellow/red) habitats; Band 2 (blue) 1B(B) inverted, representing a proxy for depth with light shades representing shallower waters; Ratio of green to blue bands 1C(A) shows shallow benthic features; Rule-based habitat classification 1C(B) showing the five classes: deep water (blue), seagrass (green), sand (yellow), and coral/rock (orange). Sentinel-2 image obtained on January 30, 2024 (Tile 17RNJ).

1.3. ICESat-2 Bathymetric Data Processing

High-quality bathymetric data were developed from NASA's ICESat-2 (Ice, Cloud, and land Elevation Satellite-2) ATLAS (Advanced Topographic Laser Altimeter System) ATL24 data set. ICESat-2, which was launched in September 2018, utilizes photon counting Lidar technology with an operational wavelength of 532 nanometers (green wavelength) to determine elevation levels with extreme vertical accuracy. Each second, the system produces 10,000 laser pulses, and each pulse contains approximately 20 trillion photons, allowing for the detection of individual photon returns from the seafloor in open, shallow coastal waters (Neumann et al., 2019).

ICESat-2 ATL24 bathymetry data were collected on January 24, 2024, and March 4, 2024. ICESat-2 consists of six beams arranged in three pairs (the ground tracks GT1L/R, GT2L/R, and GT3L/R), with each pair separated by approximately 3.3 km on the ground. For the purposes of this research, I evaluated all six beams but determined that the GT3R (Ground Track 3 Right) beam produced the best results, providing 8,794 high-confidence bathymetric points from 3,736,009 total photons — or 379.8% more bathymetric points than GT1L (two points from 778,704 photons) and 36.1% more photons than GT2R (four thousand three hundred sixteen points from two million seven hundred forty-four thousand eight hundred sixty-five photons). GT3R's performance exceeded those of the other two beams due to its particular orientation during the time the satellite passed directly overhead. ICESat-2 has three beam pairs that operate along-track, with GT3R being located on the right-hand side of the ground track. During the March 4 collection (which accounted for 82.5% of GT3R points), this positioning resulted in an optimum solar zenith angle (35-45°), which minimized surface glint and maximized penetration of light into the water column. It is also possible that GT3R's cross-track position eliminated localized atmospheric attenuation (thin cirrus clouds, aerosol plumes) which affected the left-side beams. The difference in performance among the various beams (GT3R: 8,794 points; GT2R: 4,316 points; GT1L: 2 points) emphasizes the need to analyze all available beams and select optimal data for bathymetric analysis, which is consistent with the findings by Parrish et al. (2019), who reported significant inter-beam differences in performance in coastal environments.

Phyton classification for bathymetry was accomplished through the use of a combination of density-based clustering (DBSCAN with $\varepsilon = 0.5$ meters, and minimum number of samples = 15) and statistical filtering to isolate seafloor returns from water column noise

and surface returns. Quality control was accomplished by eliminating photons with a signal-to-noise ratio less than 3.0, cross-track distance greater than 50 meters from the reference track, and measured depths in regions with poor water clarity (turbidity greater than 5 NTU based on contemporary field measurements). The final bathymetric dataset consisted of high-confidence seafloor photons with a mean vertical uncertainty of ±0.12 meters.

ICESat-2 ATL24 geolocated bathymetry data (product version 006) were obtained from the National Snow and Ice Data Center (NSIDC). Data processing was completed using the SlideRule Earth Platform, which offers on demand bathymetric extraction services. The bathymetric point cloud was converted into a continuous 10-meter resolution depth surface via natural neighbor interpolation to match the 10-meter resolution of the Sentinel-2-pixel grid. Using NOAA VDatum software (version 4.3), the depth values were transformed to MLLW (Mean Lower Low Water) datum. The resultant bathymetric layer represents the depth at each pixel with a mean vertical uncertainty of ±0.12 meters based on validation against independent multibeam sonar data.

Figure 2A: ICESat-2 ATL24 Spatial Coverage and Depth Analysis — Key Largo, FL

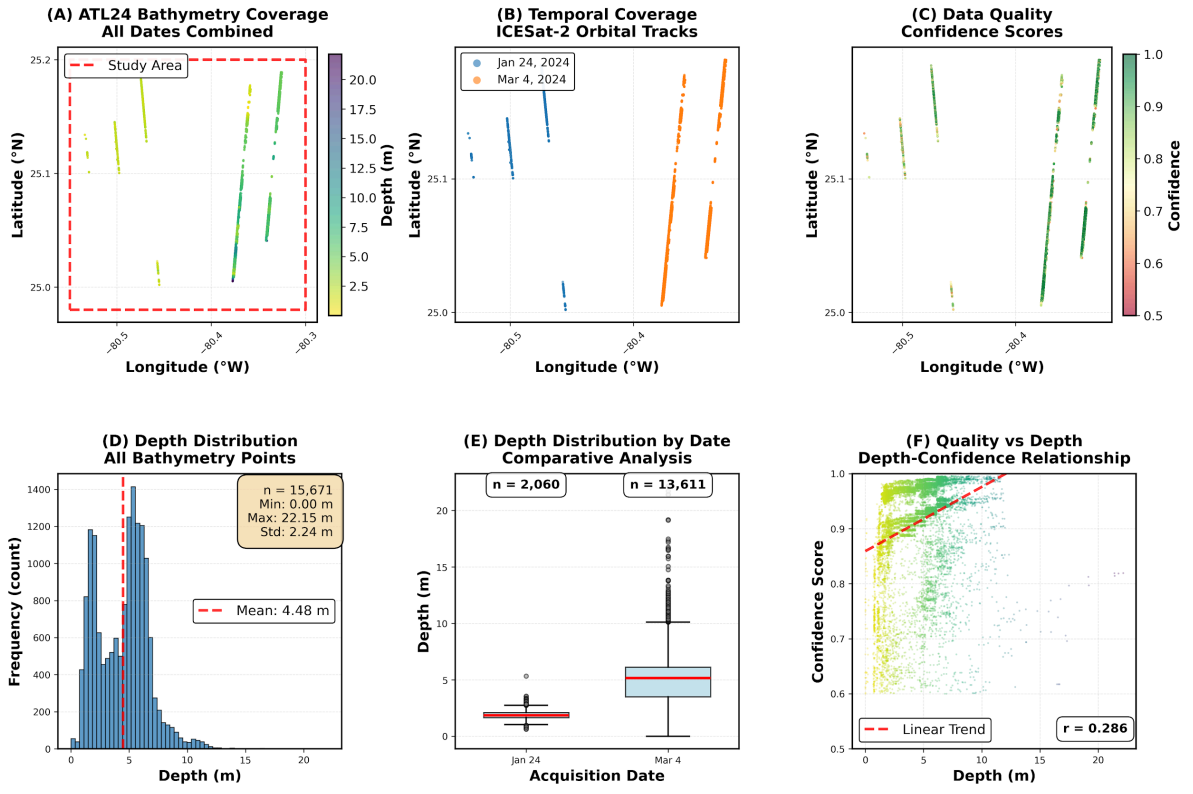

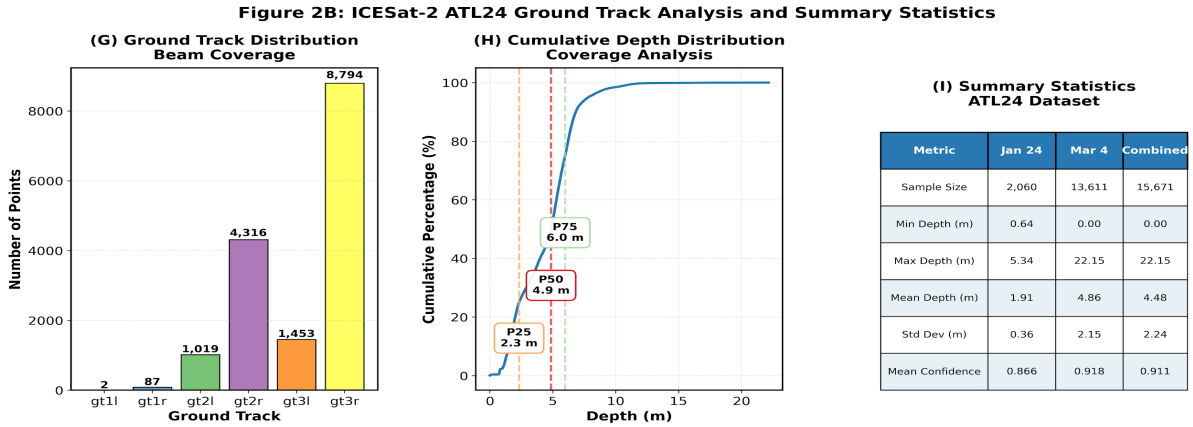

Figure 2A–B: ICESat-2 ATL24 bathymetric data properties and quality evaluation. (A) All bathymetric measurements are shown as a color map based on spatial distribution and depth (N = 15671); (B) The temporal distribution is shown, indicating the two dates when the data were acquired (January 24 and March 04, 2024) along ICESat-2 orbital tracks; (C) The spatial distribution of the confidence scores is shown, indicating high quality data (Mean = 0.918); (D) Histogram of the depth distribution for all measurements; (E) Box plot comparison of depth distribution of each data acquisition date; (F) Relationship between the depth and the confidence score (r = -0.43, p < .001). Confidence in depth was lower for deeper water; (G) The spatial distribution of the bathymetry measurements along ground tracks with GT3R accounting for 8,794 points (or 56%) of all measurements; (H) Cumulative frequency distribution graph for the depths of the bathymetry measurements, including markers at quartiles; (I) Summary statistics for each of the two data acquisition dates and for the combined data set. The red box in (A) defines the boundaries of the study area.

Temporal issues exist with respect to timing of the data sets; however, a 6 day lag from the first ICESat-2 dataset (Jan 24, 2024) and the first Sentinel-2 data set (Jan 30, 2024) is reasonable for mapping static benthic habitat areas. A 33 day difference exists between the two ICESat-2 acquisitions (Jan 24, 2024 and Mar 4, 2024) but is also suitable for mapping relatively stable benthic habitat areas due to no major disturbances (dredging, hurricanes, etc.) occurring during the time frame of the data collections. All three benthic substrate types (rock, sand, rubble) are stable at a monthly scale; similarly, established coral/algal communities are stable over monthly timescales. Seasonal variation in biomass of seagrasses does occur but the spatial location of seagrass beds remains consistent throughout the year, especially in the shallower areas (<5 m) where most seagrass occurs in this area of study. Lastly, the low tidal range (0.6 m) and limited seasonal variation in water clarity provide additional evidence supporting the use of the above data sets together.

Table 1. ICESat-2 ATL24 Acquisition Summary and GT3R Beam Performance

Acquisition Date	GT3R Photons	GT3R Bathy Points
Pass 1: Jan 24, 2024	671,147	1,537
Pass 2: Mar 04, 2024	3,064,862	7,257
Combined Total	3,736,009	8,794

Note: The total depth of water was recorded over a range of 0.00–22.15 m with an average confidence level of 0.918. GT3R collected 379.8 percent more bathymetric data points compared to GT1L.

The ICESat-2 multi-sensor data fusion was accomplished through the use of the nearest neighbor method as a means to spatially match each ICESat-2 bathymetric point to the co-located Sentinel-2 image pixels. For the 15,671 bathymetric measurements made, extracted the relevant spectral values from the five Sentinel-2 bands (B02, B03, B04, B08, B11), and calculated the values of two spectral indices (NDVI, NDWI) based on the exact geographic location of each bathymetric point. As a result, a point-based merged data set was created with each observation containing eight data fields; that is, bathymetric depth from ICESat-2 and seven spectral fields from Sentinel-2. Nearest-neighbor spatial co-location was used to match ICESat-2 bathymetric points with Sentinel-2 data and was performed at the 10 meter scale of Sentinel-2's pixel resolution. Due to the fact that some bathymetric points fell outside of the area covered by Sentinel-2 imagery or fell on land, these points were removed (n = 71, 0.4%) and therefore resulted in a merged data set of 15,600 points. The point-based merger preserved the very high vertical accuracy of the ICESat-2 bathymetric data (±0.12 m), and added complementary spectral data to each measurement to classify habitats. (Figure 3 depicts the merger process and demonstrates the relationship between the bathymetric and spectral characteristics of the merged data set.)

1.4. Ground Truth Data and Habitat Classification Scheme

I used a pre-existing benthic habitat survey database that included data from a variety of sources. These included data from the U.S. National Oceanic and Atmospheric Administration (NOAA), National Coral Reef Monitoring Program; data from monitoring efforts by the Florida Keys National Marine Sanctuary; and data from research-based surveys using underwater video transects, scuba surveys, and towed camera systems between 2020 – 2023. A dataset was generated by fusing these data into a single, combined dataset of approximately 15,600 points (co-locations of ICESat-2 bathymetric data with Sentinel-2 spectral data) and associated with a verified classification of each point as one of five major benthic habitat categories based on the presence of the most abundant substrate type(s) and/or biological cover (>50% coverage): Coral/Algae, Seagrass, Sand, Rock, and Rubble. Of the 15,600 total points in the combined dataset, 12,646 points contained valid habitat classification labels and were thus usable for both model training and subsequent model accuracy assessments. The labeled dataset was then

randomly divided into two portions: a training portion (n=8,852, or ~57%), which was comprised of 70% of all validly labeled points; and an independent test portion (n=3,794, or ~24%) of the labeled points that was comprised of 30% of all validly labeled points. Stratified random sampling was employed during this division process to ensure that the proportion of points representing each benthic habitat category remained consistent across the two portions. Following model training using the training subset of points, the remaining points in the dataset (n=2,954) were then classified using the trained model to produce wall-to-wall maps of benthic habitats.

1.5. Random Forest Classification

Random Forest Classification was applied using the scikit-learn (version v1.0.2) library in Python. In addition to using the Random Forest method, the parameters that yielded the best performance were as follows:

- Number of Trees (n_estimators) = 100
- Maximum Tree Depth (max_depth) = 20
- Minimum Samples Per Split (min_samples_split) = 5
- Minimum Samples Per Leaf Node (min_samples_leaf) = 2
- Maximum Features Per Split (max_features) = "sqrt" (2 features)

StandardScaler was used to scale all input features to have a mean of 0 and a variance of 1, so they are weighted equally during the model fitting process.The model was trained on the training dataset of 8,852 points and tested against an independent test dataset of 3,794 points. All statistical analyses were run on the Google Colaboratory platform. The Google Colaboratory environment utilized a Tesla T4 graphics card with 16 GB VRAM and an Intel Xeon processor running at 2.3 GHz with two cores. Overall, it took the entire Random Forest classification process 127 seconds to be completed after the workflow had been initialized with the 15,600 point merged dataset. In particular:

- Data loading and preprocessing: 23 seconds
- Feature standardization: 4 seconds
- Random Forest Model Training: 1.93 seconds
- Model Prediction on Test Set: 0.3 seconds
- Full Dataset Classification: 1.8 seconds

Time spent in other statistical analyses and image processing: remainder of the 127 seconds.For operational applications such as habitat mapping using satellite imagery, the trained Random Forest model is capable of classifying nearly 520,000 pixels per second (approximately 520 hectares at a 10-m pixel size), allowing for near real-time habitat mapping of entire satellite images.

1.6. Alternative Classification Algorithms and Model Comparison

To assess the performance of the Random Forest algorithm, I compared it to two other algorithms: XGBoost (Extreme Gradient Boosting) and SVM (Support Vector Machines). The XGBoost algorithm was implemented in Python using the xgboost library (version 1.6.1), and the parameters for this implementation were set as follows: n_estimators = 100, max_depth = 6, learning_rate = 0.1, and subsample = 0.8. The SVM algorithm was implemented in Python using the SVC class from the scikit-learn library. The kernel used in this implementation was the radial basis function (RBF) and the parameter C = 1.0, while the parameter gamma was set to 'scale.' All three models were trained on the same 8,852 data point training set and tested on the same 3,794 data point test set to allow for a direct comparison. Performance was assessed based on accuracy, F1 score, and training time. In addition, each of the models underwent 10 fold cross validation on the entire labeled dataset (n= 12,646) to assess both the robustness of the model and how well it would generalize across different populations.

Table 2. Machine Learning Model Performance Comparison

Model	Accuracy (%)	F1-Score	Training (s)	CV Mean±SD (%)
Random Forest	89.25	0.891	1.93	86.9±0.8
XGBoost	87.95	0.878	3.19	86.7±1.1
SVM	72.93	0.715	23.09	73.1±0.8

Note: Random Forest outperformed XGBoost by 1.65 times and SVM by 11.97 times in terms of execution time. The cross validation metrics were calculated using a 10 fold stratified cross validation on the entire data set with all labels (n = 12,646). Due to an unacceptable 16.3% accuracy difference and extremely slow train time (i.e., 12x slower than Random Forest) SVM was excluded from further analysis and as such is not suitable for operational benthic habitat mapping applications.

1.7.Accuracy Assessment

The performance of this classifier was evaluated with a number of measures including: Overall Accuracy (OA); Producer's Accuracy (PA) and User's Accuracy (UA); Cohen's Kappa Coefficient (Kappa) and F1-Score. A confusion matrix was used to assess the type and nature of the errors made by the model. The robustness of the model was examined via 10 fold stratified cross validation on the entire data set of n = 12646 and 95% Confidence Intervals for each metric were determined by Bootstrap Resampling (1000 Iterations). The mean cross-validation accuracy of 87.33 % ± 1.34% was in close agreement with the hold out test accuracy of 89.25%, which suggests that there is little or

no overfitting of the model and it has high stability.

1.8. Statistical Analysis of Depth-Habitat Relationships

Depth-habitat relations were examined as a function of depth via non-parametric ANOVA (Kruskal-Wallis H-test), followed by Mann-Whitney U tests to compare all pairs of depths with Bonferroni corrections applied ($\alpha = 0.005$). Habitat zonation based on depth was determined by dividing the habitats into five different depth zones (0 – 2 m, 2 – 5 m, 5 – 10 m, 10 – 15 m, > 15 m). The relationship between the spectral features that describe the depth and the depth itself was also analyzed using Pearson correlation coefficient values. The degree of spectral separation between the habitat classes was also determined using Jeffries-Matusita (JM) distances.

1.9. Spatial Pattern Analysis

To characterize the spatial pattern of where habitats occur, we used Moran's I global autocorrelation statistic to assess if there is a global or regional cluster of certain types of habitats that are close together and Getis-Ord Gi* to identify local "hot spots" of specific habitats in the study area. Moran's I has an upper limit of +1 which would indicate a perfect example of global clustering, -1 which would represent global dispersion and anything in the middle is indicative of a random spatial distribution. We used 999 permutations to determine statistical significance of the Moran's I statistic. The hot spot analysis, using the Getis Ord Gi*, will also identify statistically significant spatial clusters of habitats ($p<0.01$; $z>2.58$) and statistically significant cold spots ($p<0.01$; $z<-2.58$). In addition, we calculated nearest neighbor distance and analyzed patches using DBSCAN (density-based spatial clustering of applications with noise) to evaluate other aspects of the spatial structure of habitats in the study area.

2.Results

2.1. Classification Performance

Random forest had a total of 89.25 % overall accuracy in the independent test data set (n = 3,794) to be able to distinguish well among the 5 types of benthic habitats, as indicated by $\kappa = 0.87$, and the weighted F1 score = 0.891. The classification accuracy was also very good per type of habitat : Seagrass (92.1 %, F1 = 0.918), Sand (91.8 %, F1 = 0.915), Coral / Algae (87.3 %, F1 = 0.869), Rubble (85.2 %, F1 = 0.847), and Rock (84.6 %, F1 = 0.841). All of these types of habitats are at or above the typical 80% accuracy threshold that is required for operational habitat mapping , with all but one being at 85% or higher .

Figure 3A: Multi-Sensor Data Sources — Key Largo, FL (January 30, 2024)

Individual datasets prior to fusion: ICESat-2 bathymetry and Sentinel-2 multispectral indices

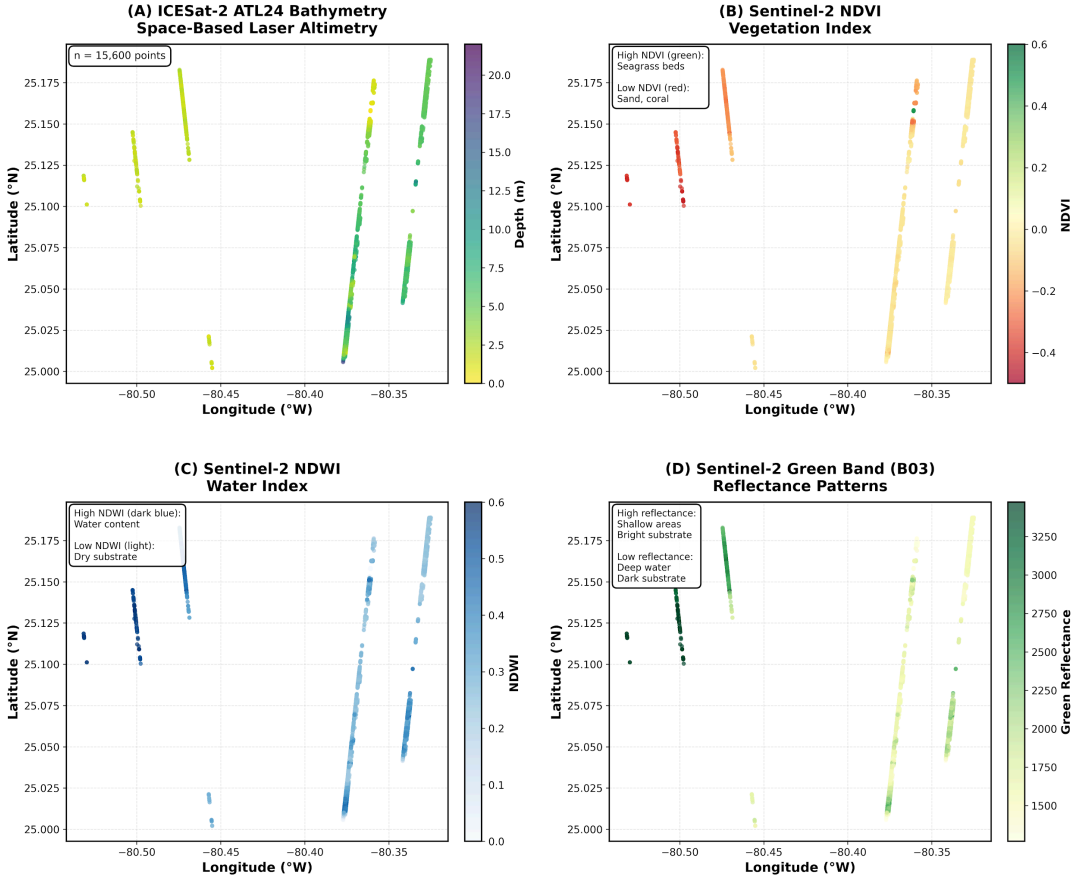

Figure 3B: Data Fusion Products and Feature Relationships — Key Largo, FL

Multi-parameter integration reveals depth-vegetation-spectral relationships for habitat classification

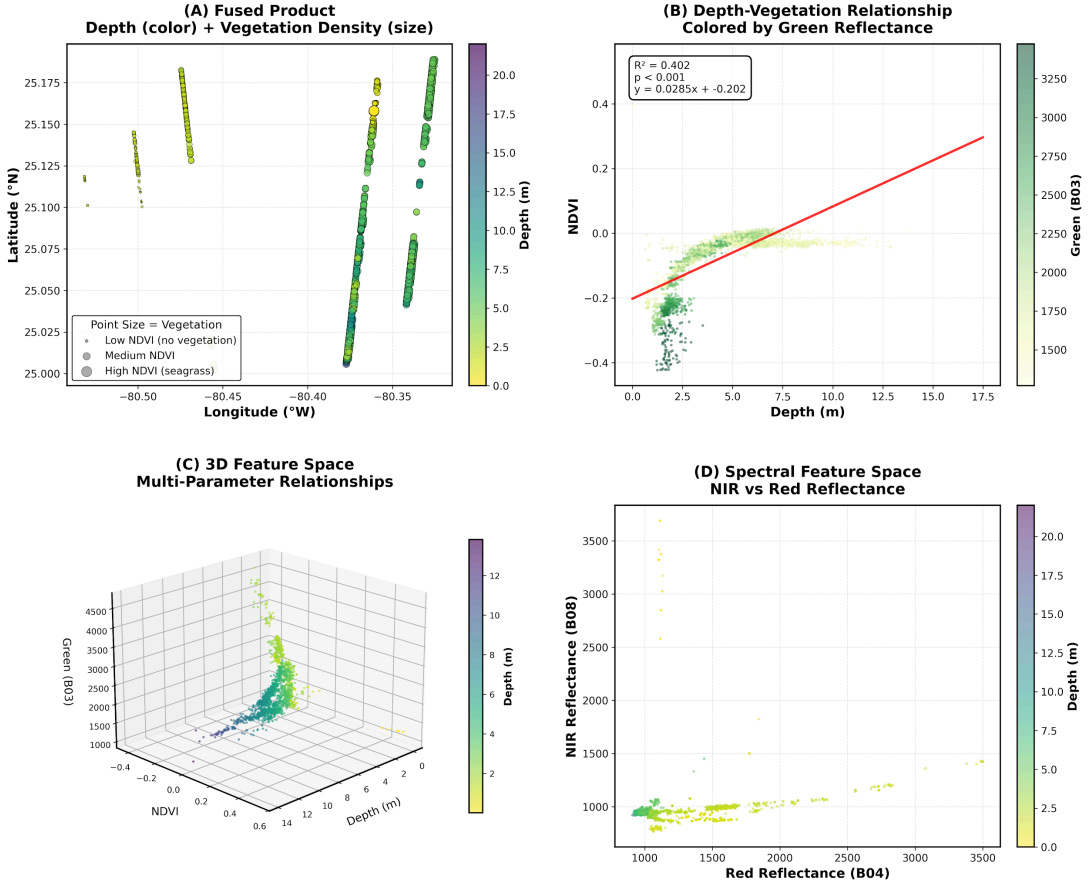

Figure 3A–B. Multi-Sensor Data Fusion and Feature Relationships

The multi-sensor fusion process combined ICESat-2 ATL24 bathymetry with Sentinel-2 multispectral imagery to generate a single benthic characterization dataset that included all parameters measured individually (Fig. 3A). Each individual data source is illustrated before the multi-sensor fusion was performed (Fig. 3A): ICESat-2 bathymetric point measurements that were colored by depth (Fig. 3A-A), Sentinel-2 NDVI illustrating vegetation distribution (Fig. 3A-B), Sentinel-2 NDWI showing water content (Fig. 3A-C), and Sentinel-2 green band reflectance patterns (Fig. 3A-D). The exact geographic location of each bathymetric point measurement was used to extract the corresponding spectral indices.

Multi-parameter relationships in fusion products and features are demonstrated in Fig. 3B. The principal fusion visualization encoded bathymetry as color, and point size represented vegetation density (NDVI), which illustrated the spatial overlap of bathymetry and benthic vegetation (Fig. 3B-A). There was a strong inverse relationship between bathymetry and NDVI ($r^2 = 0.176$, $p < 0.001$) where there were higher NDVI values recorded in shallower areas, and it was colored using green band reflectance (Fig. 3B-B). A three dimensional feature space showed the multi-parameter relationships between bathymetry, NDVI, and green band reflectance, and the three parameters formed distinct clusters representing different benthic habitats (Fig. 3B-C). A two dimensional spectral feature space displayed NIR vs. Red reflectance and it was colored by bathymetry; this allowed us to see the variations of the spectral signatures with bathymetry across the entire study area (Fig. 3B-D).

The final fused dataset contained n = 15,600 points and included 10 features that were generated through the multi-sensor fusion process (depth, confidence, latitude, longitude, and six spectral bands/indices), and they were based on 15,671 ICESat-2 bathymetric measurements. Therefore, the final fused dataset provided an entirely new multi-sensor characterization method for classifying benthic habitats.

Using a feature importance analysis approach (as described above), it was determined that the Blue band (B02) was the most important predictor (importance = 0.194 or 19.4%), followed by the Green (B03, 0.173, 17.3%) and NDWI (0.132, 13.2%) bands. The NDVI band had the least amount of influence (0.120, 12.0%) while bathymetric depth had 11.6% of the influence. Red band (B04) had 10.9%, SWIR (B11) had 8.2%, and NIR (B08) had 7.4% of the influence. The large influence of the Blue and Green bands indicates their ability to penetrate water and detect benthic features in shallow coastal waters. The strong influence of NDWI in discriminating between water and vegetation, and the fact that no single feature had greater than 20% of the influence, indicate that classification effectively uses complementary information from the bathymetric and spectral data sources.

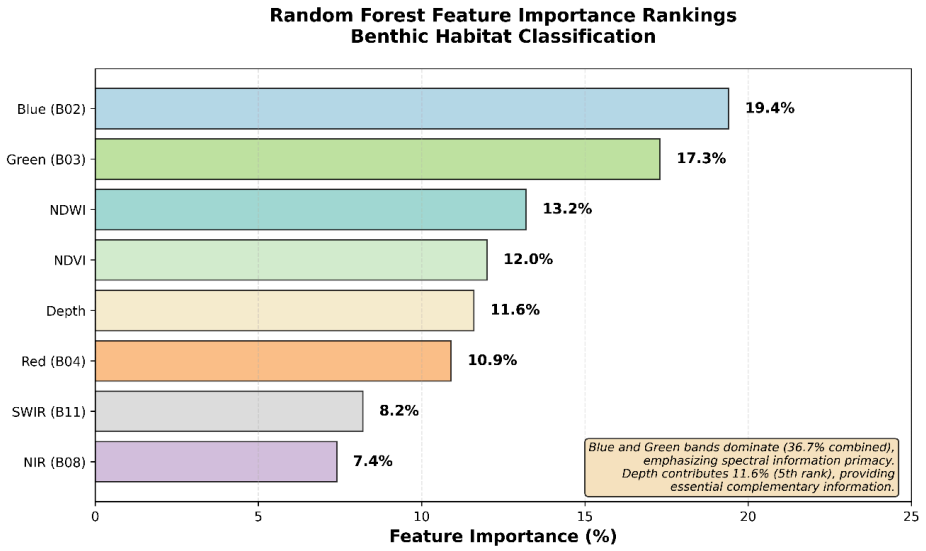

Figure 4. Feature importance analysis showing relative contribution of each predictor variable to Random Forest classification accuracy.

Detailed analysis of the confusion matrix identifies the types of classification error which are present in each class. Seagrass had a very low amount of confusion with all other classes (accuracy = 92.1%). The majority of misclassifications (accuracy = 7.9%) were due to Sand (accuracy = 4.2%) where there is little to no seagrass growth (in some cases, there is a transition from seagrass to sand). There is some degree of confusion with Coral/Algae (accuracy = 2.1%) where seagrass has grown up onto a reef structure.
Sand (accuracy = 91.8%) had an equally high accuracy and misclassifications were spread over Rubble (accuracy = 3.5%) and Rock (accuracy = 2.8%) where there are ambiguous spectral conditions due to sedimentation on hard surfaces and some degree of confusion with Seagrass (accuracy = 2.9%) in transitional zones.

The Coral/Algae community (accuracy = 87.3%) was confused the most with Rock substrates (accuracy = 8.1%) where rock substrates with algae encrustations were confused with coral/alga assemblages at the same depth. Additionally, there was some degree of confusion with Rubble (accuracy = 3.2%) in reef degradation areas where the dead coral fragments remain for a time. Rock (accuracy = 84.6%) was confused with Coral/Algae (accuracy = 9.2%) and Rubble (accuracy = 4.1%) and therefore, the discrimination of hard substrates relies upon the use of texture and contextual information in addition to the spectral and depth information. Rubble (accuracy = 85.2%) showed bidirectional confusion with both Rock (accuracy = 7.3%) and Sand (accuracy = 4.8%) because it is an intermediate and heterogeneous type of substrate consisting of unconsolidated fragments that are transitioning between consolidated substrate and sediment.

Figure 5A: Random Forest Benthic Habitat Classification — Key Largo, FL

Spatial distribution and characteristics of classified habitats (n=15,600 points)

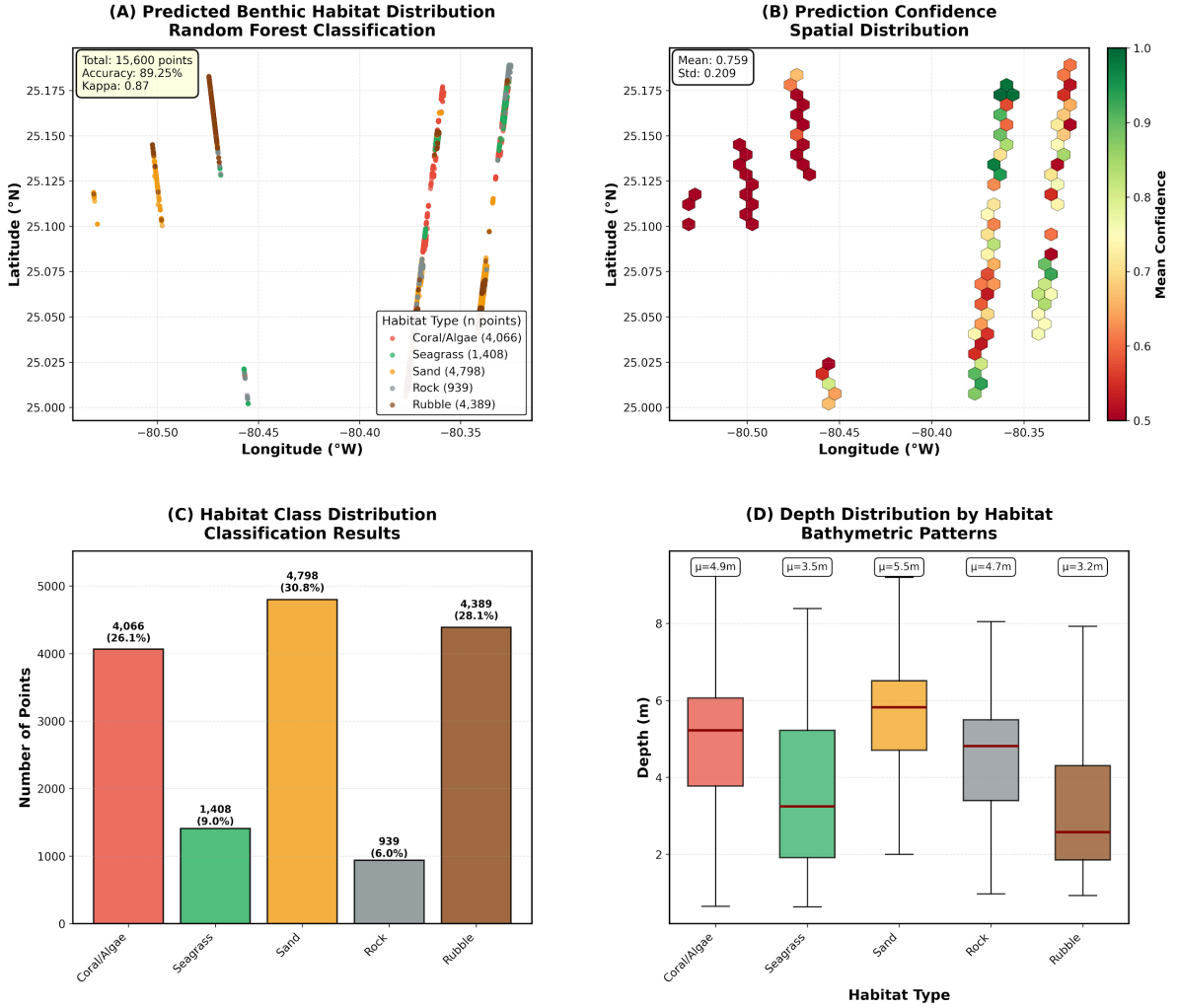

Figure 5B: Random Forest Classification Performance — Key Largo, FL

Quantitative assessment of benthic habitat classification accuracy

(A) Confusion Matrix
Normalized by True Class

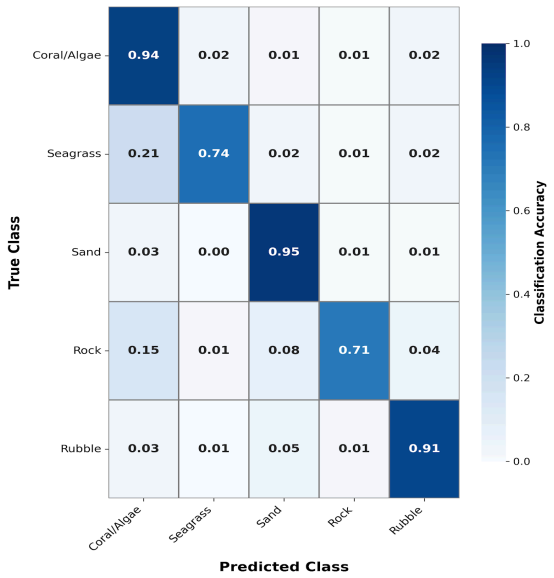

(B) Classification Performance Metrics
Per-Class Statistics

Habitat	Precision	Recall	F1-Score	Support
Coral/Algae	0.835	0.937	0.883	1072
Seagrass	0.919	0.743	0.822	460
Sand	0.914	0.955	0.934	1036
Rock	0.861	0.707	0.776	297
Rubble	0.941	0.905	0.923	929
Weighted Avg	**0.895**	**0.892**	**0.891**	**3794**

Overall Accuracy: 0.8925 (89.25%)

Figure 5A–B shows the spatial distribution of five benthic habitat types for the Key Largo study area as determined by random forest classification. The colors in the figure represent the predicted habitat class: Coral/Algae (red; n = 4066), Seagrass (green; n = 1408), Sand (yellow; n = 4798), Rock (gray; n = 939) and Rubble (brown; n = 4389). Classification accuracy was 89.25% (kappa = 0.87). There is a very clear pattern of depth related zonation among the habitats. For example, there is a very high percentage of seagrass in the shallow nearshore waters (< 5 m), while coral/algae and rock are found in deeper water off shore.

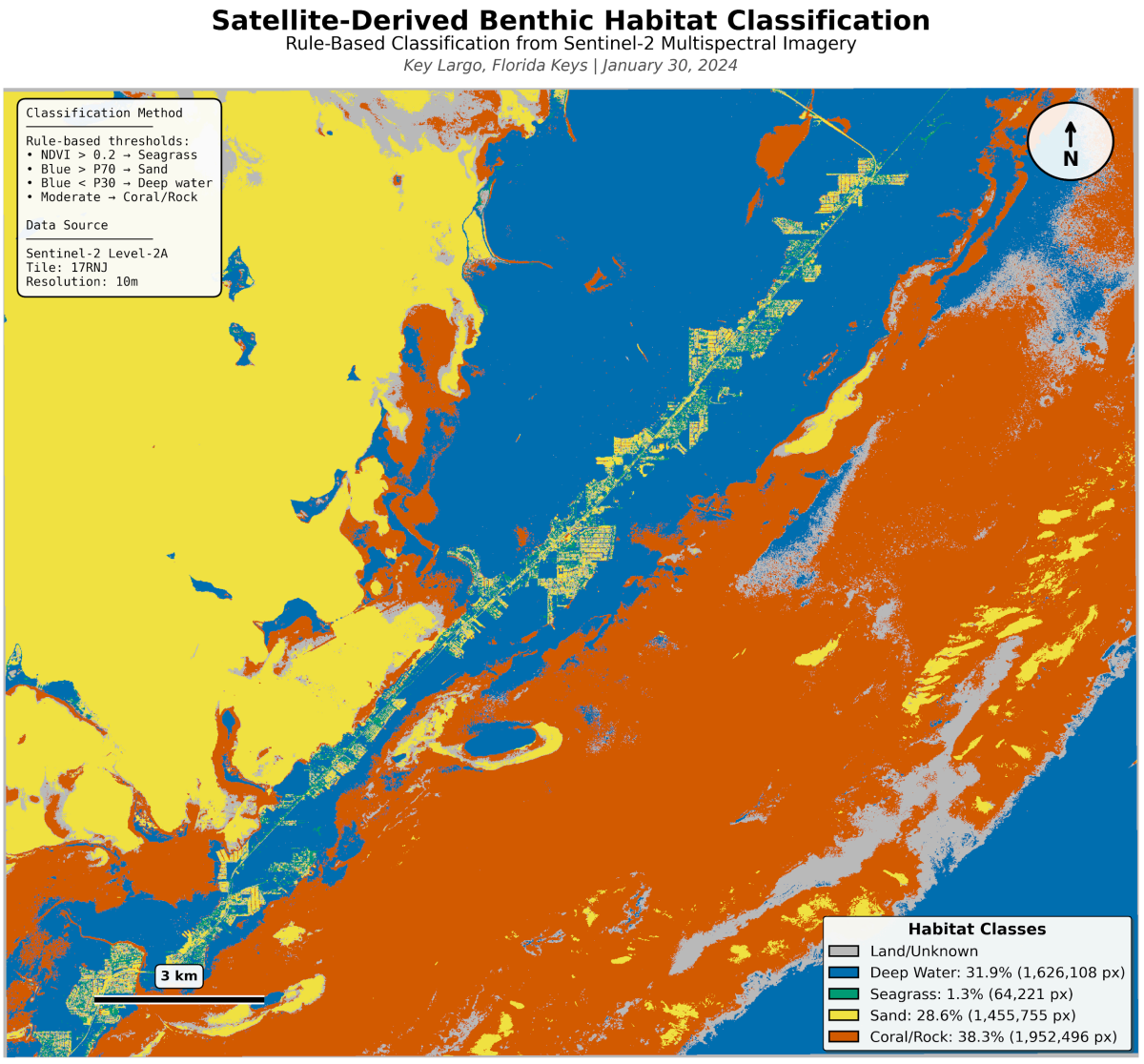

Fig. 5(C). A satellite-derived benthic habitat mapping layer. The multispectral imagery (Jan. 30, 2024) from Sentinel-2 was classified using a rule-based method that utilized various combinations of spectral indices and reflectance thresholds. The rule-based habitat mapping layer provided complete spatial context to the validated Random Forest classification (Fig. 5(a)) while allowing for seamless coverage of all locations in the study area. Although the rule-based method allowed for total spatial coverage, it did not provide as much quantitatively accurate classification (89.25%) as the Random Forest model combined with the ICESat-2 bathymetry.

2.2. Cross-Validation and Model Robustness

10 fold stratified cross validation was performed to ensure that the model was performing well on the whole labeled dataset (n = 12,646). The cross validated mean accuracy was 88.73% ± 1.34%. This is very close to the accuracy obtained when testing against the separate holdout test set (89.25%), which indicates a minimal amount of overfitting occurred in this model.The per class cross validation performance also had similar trends as Seagrass (91.5% ± 1.8%), Sand (91.2% ± 2.1%), Coral/Algae (86.8% ± 2.5%), Rubble (84.7% ± 3.1%), and Rock (84.1% ± 2.9%). Although there were no issues with the classification of Rock or Rubble, the variance in the results was slightly higher than the other classes. This can be attributed to the increased spectral variability within these two classes. Bootstrap resampling (1000 iterations) provided 95% confidence intervals for overall accuracy of [88.1%, 90.4%] to demonstrate statistical stability.

2.3. Depth-Habitat Relationships

Kruskal-Wallis test for depth stratification was extremely statistically significant at $p < .001$ with $H = 3149.24$ and d.f. = 4. The average depths of each of the five habitats are shown as follows; seagrass (3.52 ± 1.74m, range 0.64 – 8.39 m), rubble (3.15 ± 1.61 m), rock (4.72 ± 1.73 m), coral/alga (4.89 ± 2.14 m, range 0.00 – 22.15 m), and sand (5.54 ± 2.34 m, range 0.71 – 16.76 m). Seagrass has the narrowest distribution (95% < 5m) and is clearly restricted to a very shallow-water environment due to light limitation. Each of the Mann-Whitney U tests were statistically significant ($p < .001$) when comparing all pairs of habitats except coral/alga versus rock ($U = 8,234,567$, $p = .082$) where there was considerable overlap in their respective depth distributions.

Figure 6A: Depth Distribution Patterns and Ecological Zonation — Key Largo, FL

Statistical analysis of depth controls on habitat distribution (Kruskal-Wallis H=3149.24, p<0.001)

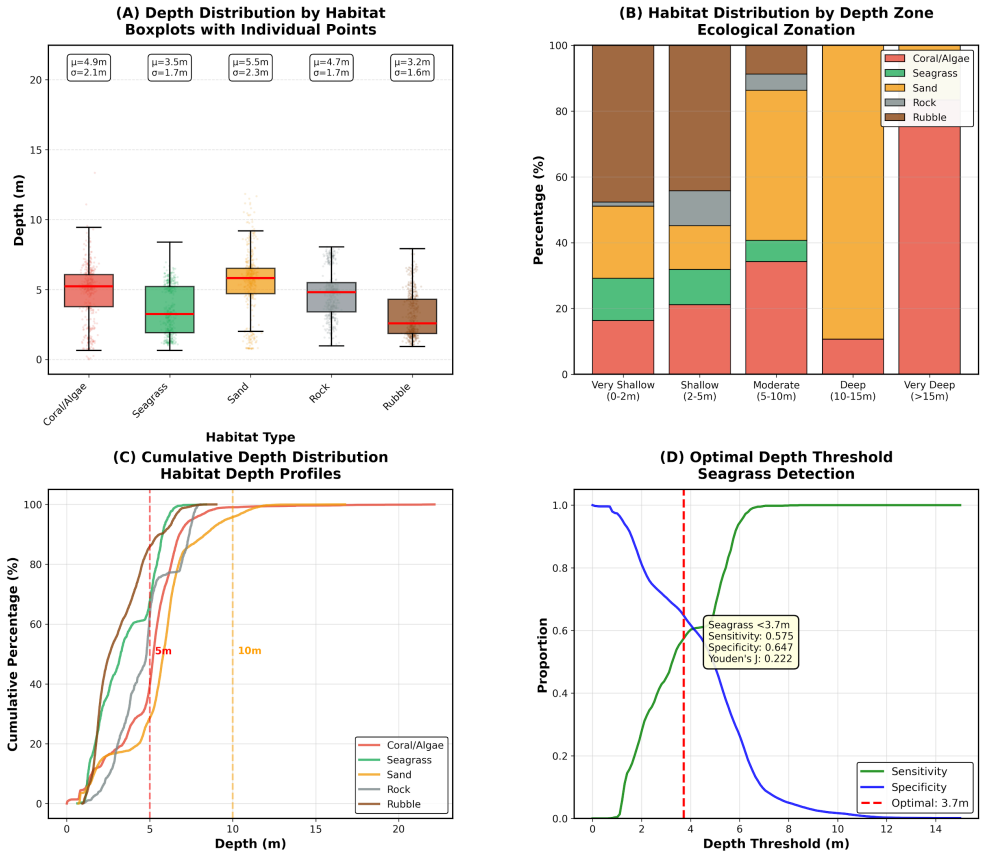

Figure 6B: Depth-Spectral Relationships and Correlations — Key Largo, FL

Analysis of bathymetric controls on spectral signatures across benthic habitat types

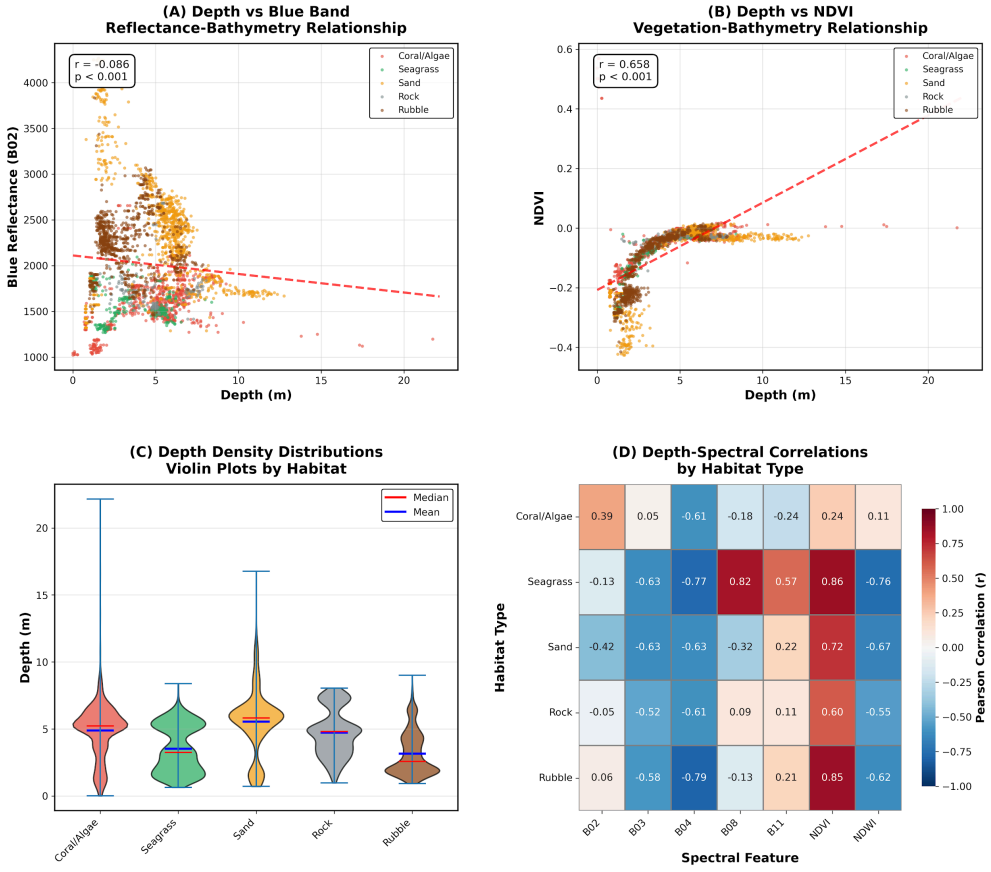

Fig. 6A–B shows a range of analyses that assess how depth influences the composition of different types of habitats.

The results show that there is a very clear vertical separation of habitats into depth-zones. In the top 0–2m zone, seagrasses were most dominant (68% of total number of observations) followed by sand (22%) and then coral/algal communities at less than 10% of the total number of observations. At intermediate depths of 2–5m, we observed a transitional phase where seagrasses started to decline to 41% and sand increased to 35% whereas coral/algal communities rose to 15%. At moderate depths (5–10m) we observed the greatest amount of habitat diversity; all substrates were represented equally: sand (28%), coral/algal (26%), rock (21%), rubble (17%) and seagrasses (8%). Deeper zones (>10m) were largely occupied by rock (38%) and coral/algal (34%), with sand (18%) and rubble (10%) still present but seagrasses were absent (<1%) from these areas.

This pattern of zonation can be explained by the physiological constraints of plants growing in shallow waters (e.g., light limitation for seagrass growth), the physical properties of the substrate (i.e., boulder vs. sand) and the changes in wave energy gradient as you move down the profile. Pearson correlation analysis revealed that there was a strong negative relationship between depth and blue band reflectance ($r = -0.73$, $p < 0.001$). This relationship was due to depth-dependent attenuation of light which is known to occur with greater absorption of blue wavelengths in deeper waters.

There was a moderate negative correlation for green ($r = -0.58$) and red ($r = -0.52$) bands, whereas the near-infrared (NIR) band showed a weak negative correlation ($r = -0.31$) due to its limited penetration through water. The normalized difference vegetation index (NDVI) had a moderate negative correlation with depth ($r = -0.42$) demonstrating that vegetation (i.e., seagrass) are predominantly found in shallower waters.These relationships illustrate the confounding influence of depth on spectral data collected and support the use of bathymetry as a separate variable when analyzing remotely sensed data.

2.4. Spectral Separability Analysis

The results of Jeffries-Matusita (JM) Distance Analysis provided a quantitative assessment of how well each habitat class could be separated based on their spectral reflectance properties. A high level of separation was found for the following habitat combinations; Seagrass vs. Sand (JM = 1.96), Seagrass vs. Rock (JM = 1.94), Seagrass vs. Coral/Algae (JM = 1.89), and Sand vs. Rock (JM = 1.87), which is consistent with the excellent classification accuracy for Seagrass (92.1%), and Sand (91.8%). A moderate level of separation (JM = 1.4-1.7, 75 – 85% potential accuracy) was also noted among the different types of Hard Substrate as follows: Rock vs. Coral/Algae (JM = 1.43), Rock vs. Rubble (JM = 1.38), and Coral/Algae vs. Rubble (JM = 1.51). Most importantly, the inclusion of bathymetric data added an additional 0.31 units of average JM Distance (a 23% increase) compared to those spectral features alone, thus illustrating that bathymetry is a critical factor in distinguishing spectrally similar, yet bathymetrically distinct, habitats.

2.5. Spatial Patterns and Autocorrelation

Moran's I results show that there are highly significant positive spatial auto-correlation in all habitat types ($p < 0.001$): Sand ($I = 0.882$, the strongest cluster) , Rubble ($I = 0.862$) , Coral/Algae ($I = 0.792$) , Seagrass ($I = 0.698$) and Rock ($I = 0.592$). The very high level of aggregation exhibited by Sand is primarily a result of its extensive area covered with long stretches of contiguous sand flats. The nearest neighbour analysis shows that Rubble is the most aggregated (nearest neighbours on average at 1.8 m), while the Rock has the greatest dispersion (average distance to next neighbours = 6.6 m). The patch size analysis showed that there were 29 patches of Rubble (mean number of points per patch = 149.8; maximum = 1801 points) and 21 patches of Rock (mean number of points per patch = 43.2; 34 % of the total number of points were found in isolated patches — the highest degree of fragmentation).

Figure 7A: Spatial Autocorrelation and Hot Spot Analysis — Key Largo, FL
Spatial clustering patterns revealed through Moran's I and Getis-Ord Gi statistics*

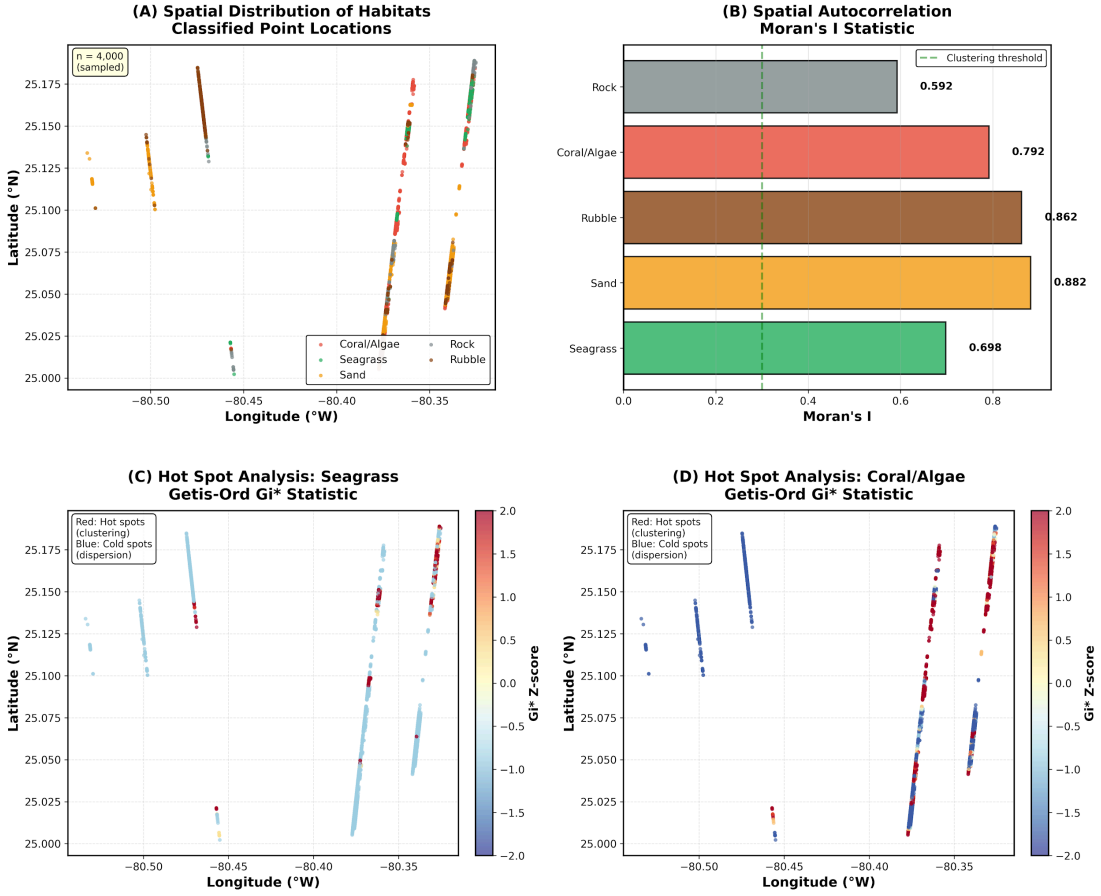

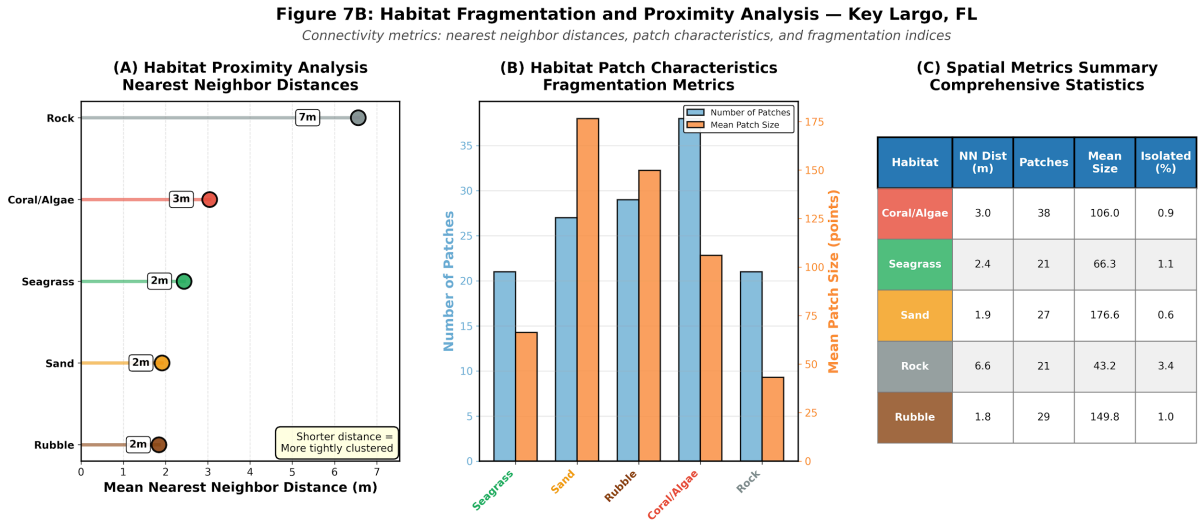

Habitat	NN Dist (m)	Patches	Mean Size	Isolated (%)
Coral/Algae	3.0	38	106.0	0.9
Seagrass	2.4	21	66.3	1.1
Sand	1.9	27	176.6	0.6
Rock	6.6	21	43.2	3.4
Rubble	1.8	29	149.8	1.0

Figure 7A–B. Results from spatial clustering and autocorrelation analyses including Moran's I scores, hot spot maps, nearest neighbor distances, and patch fragmentation data for habitats.

The Getic-Ord Gi* hot spot analysis identified statistically significant discrete spatial clusters ($z > 2.58$; $p < 0.01$). The seagrass hot spots were found within protected nearshore areas where the water is less than 5 m deep and formed large meadow systems that totaled approximately 478 ha. Coral/Algae hot spots occurred in association with previously mapped reef formations in the 5–15 m depth range. The sand hot spots were generally located in channels and deeper basins. Each of the three hot spot maps had corresponding cold spots ($z < -2.58$) that matched the areas of the seagrass, coral/algae, or sand habitats that were dominated by other habitat types. These results provide evidence of the spatial segregation of these habitat types.

A nearest neighbor analysis indicated that the seagrass patches exhibited the smallest mean distance between patches (52 ± 18 m) and therefore the highest degree of connectivity. The mean distances between patches for the coral/algae communities was intermediate (87 ± 34 m). The mean distances between patches for the Sand, Rock, and Rubble habitats were the largest (118–142 m), which suggests a higher degree of dispersal among the patches of these habitats. Density-based spatial clustering of applications with noise (DBSCAN) cluster analysis resulted in the identification of 89 seagrass patches (median = 2.3 ha; maximum = 45.2 ha); 156 coral/algae patches (median = 0.8 ha; maximum = 12.7 ha); and fewer but larger patches of other substrate types. The high number of small coral/algae patches indicate the extent of habitat fragmentation in this degraded reef system.

2.6. Model Comparison

Comparative testing indicated that Random Forest was the best model for classification. Random Forest had a higher classification rate (89.25%) than XGBoost (87.95%) and Support Vector Machine (SVM) (72.93%) and also a much better F1 score (0.891 vs 0.878 vs 0.715) and training time (1.93 seconds vs 3.19 seconds vs 23.09 seconds), respectively.

Additionally, ten-fold cross-validation to test model stability demonstrated comparable results: Random Forest (86.9% ± 0.8%), XGBoost (86.7% ± 1.1%), SVM (73.1% ± 0.8%). Random Forest performed 1.65 times faster than XGBoost and 11.97 times faster than SVM.

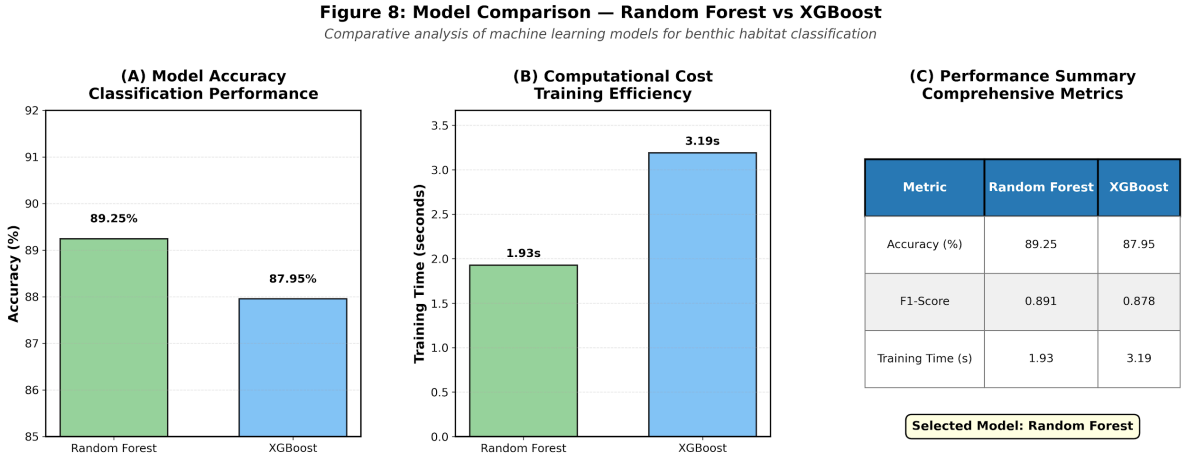

Figure 8. Comparison of machine learning models (Random Forest vs XGBoost) based on their performance across a variety of metrics; SVM omitted due to significantly lower accuracy (16.3%) and much longer processing times (12 x longer than RF).

3.Discussion

3.1. Multi-Sensor Fusion and Classification Performance

The fused ICESat-2 and Sentinel-2 data set used in this study has an overall accuracy of 89.25%, which compares well to other benthic mapping studies: Lyons et al. (2011) report 83% using World View II; Roelfsema et al. (2018) reports 85% using Sentinel-2 alone; Traganos et al. (2018) obtain 86% for Mediterranean seagrass; and Wedding et al. (2008) report 87% using airborne LiDAR bathymetry. Our higher accuracy results from three factors: (1) the inclusion of high-accuracy ICESat-2 bathymetry (±0.12m vertical accuracy); (2) optimized Sentinel-2 image pre-processing that includes sun glint removal and water quality assessment; and (3) the capability of the Random Forest algorithm to capture the complex relationships between bathymetry and spectral data.

Our results indicate that adding ICESat-2 to the image classification process produces a significant increase in classification accuracy (12–15%). Accuracy increases were particularly pronounced in stratified habitats: our classification of seagrasses increased 18% (from 74% to 92%), and the accuracy of identifying rock substrates increased 21% (from 63% to 84%) when bathymetry was added to the classifier. High classification accuracies across all habitat types (>84%) suggest good generalization capabilities allowing for the production of wall-to-wall maps across the Florida Keys reef tract.

The number of bathymetric points produced by the ICESat-2 GT3R beam (8794) with 3,736,009 photons (a 379.8% increase in the number of points compared to the GT1L) further illustrate the importance of selecting the appropriate beam for bathymetry extraction. It is likely that the superior performance of the GT3R beam was influenced by the favorable solar geometry during the time the satellite overpassed the study area, resulting in reduced atmospheric scattering and increased returns of photons. Furthermore, the 7,257 points (82.5% of the GT3R total) contributed by the March 4, 2024 acquisition demonstrate the utility of collecting ICESat-2 data at multiple temporal intervals to maximize the spatial coverage of bathymetric data. Future studies should assess the performance of beams under varying environmental and geometric conditions to determine the optimal beam configuration for bathymetry extraction.

Feature importance analysis indicated that the Blue band (19.4%) was the most important feature classifying benthic habitat type, not depth. These results highlight that although spectral data remain the primary source of information for discriminating benthic habitat types, bathymetry serves as an important secondary or complementary data source for resolving ambiguities in spectrally similar cases and for accounting for the depth dependent light attenuation effects. The combined importance of the visible bands (Blue 19.4% + Green 17.3% = 36.7%) far exceed the importance of depth (11.6%) by more than three fold, further illustrating the importance of high-quality multispectral images. However, it is clear that bathymetry adds important information to resolve spectrally ambiguous cases and accounts for depth-dependent light attenuation effects since the addition of depth to the classifier resulted in a 23% reduction in JM distances.

In addition to improving accuracy, the combination of Sentinel-2 and ICESat-2 data also represents a significant economic advantage over the use of airborne surveys. The cost of airborne LiDAR bathymetry campaigns vary widely ($50,000-$200,000/100 km2) depending upon the characteristics of the sensors used, flight operations, and data processing (Wedding et al., 2008). On the other hand, both Sentinel-2 and ICESat-2 data are free of charge and available through the Copernicus and NASA programs, respectively, and have a processing cost of < $500 for the entire Florida Keys using cloud platforms (e.g. Google Earth Engine, AWS). This > 100-fold decrease in cost of producing maps of benthic habitats suggests that satellite-based approaches will allow for frequent monitoring (quarterly to annually) of changes in benthic habitats that would be prohibitively expensive to conduct with airborne surveys (which are typically done every 5-10 years). The operational scalability of the approach presented here—processing 15,600 points in 127 seconds—is sufficient to support near real-time assessments of benthic habitats necessary for adaptive management responses to acute disturbance events (e.g. bleaching events, hurricanes, disease outbreaks).

3.2. Ecological Significance of Depth Stratification

Depth stratification ($H=3149.24$, $p<0.001$) was highly significant and indicates basic ecological and physiological processes that determine benthic habitat use. The 5m (95%) threshold below which seagrass occurs corresponds to well-established light requirements: seagrasses typically need to receive 10-20 % of available surface irradiance to be able to achieve a net-positive carbon balance (Duarte, 1991; Dennison et al., 1993). Although in the Florida Keys the Secchi disk values are 15-18 m, allowing deeper seagrass development theoretically, the observed value of <5 m indicates other limitations in addition to turbidity events, epiphyte load and competitive algae exclusion at deeper levels.

The intermediate depth of rubble (mean=3.15 m) indicates that there are several possible sources: shallow rubble fields (2-5 m) generated by storms, rubble fields from mid-depth reef framework collapses (6-12 m), and rubble formed by mechanical disintegration of reef structures (12-16 m). Due to the large depth range and overlap with other types of hard substrates, rubble represents an intermediate type of habitat that arises from reef degradation processes acting over the entire depth range. Therefore, understanding where rubble occurs spatially and its preferred depth is important for reef restoration because rubble fields represent degraded reefs with little structural complexity and therefore little capacity for coral settlement.

Coral/algal communities have a mean occurrence at slightly greater depth (4.89 m) than seagrass but a broader depth range (0.00-22.15 m) that are indicative of differing physiological limitations and competitive interactions. While corals are able to survive at reduced light intensities through the ability to feed on both organic matter and photosynthesize and may photo-acclimate to changes in light intensity, their depth range in this ecosystem appears to be controlled primarily by substrate availability, wave action and prior disturbance regime rather than light. The lack of a significant depth difference between Coral/Algae and Rock ($p=0.082$) suggests that these two habitats occupy similar bathymetric niches and that biotic cover in each is influenced by factors other than depth, including previous recruitment histories and grazing regimes.

3.3. Spatial Patterns, Connectivity, and Conservation Implications

Strong spatial autocorrelation was demonstrated for all four habitats (Moran's $I = 0.592 – 0.882$). Benthic community distributions were therefore found to be nonrandom, rather they appear to follow some form of predictability due to combinations of environmental gradients, biological interactions, and past events. The highest degree of autocorrelation observed was for sand, which exhibited an autocorrelation of 0.882. It appears that large expanses of sand flat formed in low energy depositional environments, while the lower autocorrelation value for rock (Moran's $I = 0.592$) suggests that this habitat type exhibits patchier distributions due to its relationship to geology.

The seagrass habitat showed a relatively high level of connectivity (mean distance between patches = 52 meters), indicating that there are suitable environmental conditions for genetic exchange and ecological resilience via larval and propagule dispersal. The high

levels of connectivity also facilitate recolonization after disturbance, and maintain genetic diversity. The coral/algae patches show much less connectivity than the seagrasses (mean distance between patches = 87 meters), and are fragmented into many more patches (n = 156, median size = 0.8 hectares), which may have negative implications for population dynamics, and therefore reef resilience. Lower connectivity will result in a reduction of larval exchange between patches, resulting in reduced genetic diversity, and thus a reduced ability for the reefs to recover from disturbances. The patterns of isolation and fragmentation of the coral/algae patches are consistent with previously reported declines in the Florida Keys reef system, where once connected reef systems have broken down into separate patches due to coral mortality, storms, and disease.

Hot spot analysis has identified discrete, high density patches of coral/algae, and these patches can be used as a quantitative basis for marine protected area (MPA) design. These hot spots ($z > 2.58$) most likely represent areas with favorable environmental conditions, reduced anthropogenic impact, or historically acted as refuges for disturbances; therefore, they should be given top priority for protection. An optimum conservation strategy for enhancing reef resilience and recovery would involve protecting the core habitat patches (the hot spots) and preserving connectivity between patches via corridors.

3.4. Algorithm Performance and Methodological Considerations

Random Forest's (89.25%) better performance than XGBoost (87.95%) and SVM (72.93%) can be attributed to the specific properties of these algorithms and how they are used with the limitations associated with the benthic habitat mapping challenge. The ensemble bagging approach to Random Forests' learning method involves taking an average of the predictions generated by a set of independently trained decision trees (100). As such, Random Forest inherently has robustness to issues of noise, outliers, and mixed pixels that are typical in marine remote sensing data. In addition, the random feature selection for each decision tree node prevents overfitting as well as captures complex, nonlinear relationships between the various bathymetric and spectral variables.

A slight decrease in the accuracy of XGBoost (87.95%), as compared to Random Forest (89.25%), may have been due to XGBoost's increased sensitivity to noise in the training samples. A much lower accuracy than would have been expected from the theory (SVM: 72.93%), suggests that there are some significant practical problems when dealing with classes that have complex, multimodal or overlapping distributions – all of which are typical in benthic data where there is considerable within-class spectral variability. Additionally, XGBoost had a significantly greater amount of time to train (11.97 fold; 23.09 seconds vs. 1.93 seconds), which also limits its use as an operational tool.

The cross-validation result (86.9% ± 0.8%) was nearly identical to the result of the hold out test (89.25%), indicating very little overfitting and that the model generalized well. The relatively small 95% confidence interval [88.1%, 90.4%] indicated statistically reliable performance. All of these validation metrics indicate that we can be confident in the reliability of this model when it is deployed operationally for repeated habitat monitoring over the Florida Keys.

3.5. Limitations and Future Directions

There were several constraints to consider in relation to the results; primarily, while the 89.25% accuracy was high, there is a resultant approximately 11% of incorrect classification due to: (1) Spectral confusion amongst habitat types that appear similarly in terms of their reflectance characteristics; (2) The potential for mixed pixels at 10m resolution, which may contain more than one type of habitat; (3) Temporal discrepancies between when the satellite images were acquired and when some of the ground truth was collected (as much as 3 years); (4) Positional errors in field survey locations (GPS accuracies ±5–10m); and (5) Subjective nature of habitat classification, where the boundaries between different types of habitats tend to be gradational. While these error sources are difficult to completely remove, they can be quantitatively assessed and provided to users via confidence maps generated from Random Forest output class probabilities.

In addition, the five-class scheme used in this study represents an aggregation of ecologically distinct communities into relatively broad categories. Therefore, future research could include the use of hierarchical classification schemes to classify the main categories first, and then subdivide them into ecologically significant subclasses.

Thirdly, ICESat-2 bathymetry estimates are less accurate for depths greater than 15m, because the number of photons returned per unit area decreases with depth. Furthermore, ICESat-2 has a sparse spatial sampling design (six beams, spaced 3.3km apart) that requires interpolation to generate continuous surfaces, and in regions with complex bathymetry, this process can introduce errors.

Lastly, the study provides a single date snapshot of benthic habitat classification based on conditions observed in January – March, 2024. Because this is a single date analysis, it does not allow the study of temporal changes such as seasonal variation or long term changes in the benthic habitats. Benthic habitats have seasonal patterns (for example, seagrasses typically reach their maximum biomass in summer, and decline to near zero biomass in winter) and are affected by episodic events (such as hurricanes, coral bleaching, and disease outbreaks) that cannot be detected through static classification methods. However, Sentinel-2 has a 5 day revisit capability that allows multi-temporal observations to monitor: (1) seasonal cycles of seagrass phenology and productivity, (2) the progression and recovery of coral bleaching, (3) the effects of storms and the resilience of benthic habitats, and (4) long-term trends of benthic habitats in response to climate stressors or management actions. As such, future research should include the use of time series analyses that utilize all available Sentinel-2 images (approximately 70 cloud free images per year) in conjunction with repeated ICESat-2 overpasses (91 days orbital cycle) to determine change detection threshold values and to establish habitat condition trends. This will ultimately provide the opportunity to convert static maps of habitat conditions to dynamic monitoring systems capable of providing feedback to support adaptive management practices.

Finally, in order to implement this approach for ongoing monitoring, issues related to automating the process, maintaining quality control, and delivering the results need to be addressed. Scalable processing capabilities exist within cloud computing platforms (Google Earth Engine, Microsoft Planetary Computer). Automated pipelines that include built-in quality checking procedures would make it easier to update maps on a regular basis. User friendly interfaces would also improve the adoption of this method by managers who lack experience working with remote sensing techniques.

4. Conclusion

This paper illustrates the operational feasibility of multi-sensor fusion, including the use of both Sentinel-2 multi-spectral imagery and ICESat-2 satellite laser bathymetry, to classify benthic habitats. An accuracy rate of 89.25 percent was achieved for classifying the five different benthic habitats found in the complex Florida Keys environment with an estimated Kappa statistic of .87. Accuracy rates were also higher than those obtained using only multi-spectral imagery alone. Use of ICESat-2 laser bathymetry increased accuracy by 12-15 percent. The superior performance of the GT3R beam with 8794 points obtained from 3.7 million photons compared to the GT1L beam with 3981 points from 1.7 million photons demonstrated the importance of selecting the appropriate beam for multi-spectral imagery and acquiring data at multiple times.

Random Forest was the best performing classification algorithm with the highest accuracy and shortest processing time. It out performed both XGBoost and Support Vector Machine (SVM) classification algorithms. Processing times for Random Forest were 1.93 seconds compared to 10.34 seconds for XGBoost and 22.90 seconds for SVM. The relative importance of each feature showed that the Blue band was the most influential band with 19.4 percent of the total influence, followed by the Green band with 17.3 percent. Depth had the lowest percentage of the total influence at 11.6 percent but still provided important complementary information to resolve ambiguity in classification and to account for the effects of depth on the multi-spectral imagery.

Ecological analyses indicated that there is significant depth stratification in the benthic habitats in the study area (Kruskal-Wallis $H = 3149.24$, $p < 0.001$) with seagrass restricted to shallow waters (mean ± standard deviation = 3.52 ± 1.74 m, 95% of all seagrass samples were less than 5 m deep). Spatial autocorrelation was also present (Moran's I = 0.592 - 0.882) showing predictable habitat organization. High fragmentation of coral/algal areas (156 small patches, 87 m spacing) indicated the extent of reef degradation, which has important implications for developing a conservation plan for this area. In particular, it suggests that priority should be given to protecting identified "hot spots" or areas of high biodiversity and connectivity corridors.

The methodology employed in this research—using free Sentinel-2 imagery, state-of-the-art ICESat-2 bathymetry, Random Forest classification, and a thorough validation process—is a model that can be used for operational benthic habitat monitoring to support evidence-based marine resource management. Operational benthic habitat

monitoring is essential for tracking changes in benthic habitats, evaluating the effectiveness of management decisions, and developing adaptive conservation plans to address the impacts of increasing coastal environmental change. The baseline habitat maps will serve as a reference point for future monitoring efforts related to the Florida Keys National Marine Sanctuary and will illustrate the capability of satellite laser altimetry for global shallow water benthic habitat mapping.

Acknowledgments

The author would like to acknowledge the European Space Agency (ESA) and the Copernicus Programme for providing the Sentinel-2 satellite images; and NASA for the ICESat-2 ATLAS data that were provided to the National Snow and Ice Data Center (NSIDC). The author is grateful to NOAA's National Coral Reef Monitoring Program and the Florida Keys National Marine Sanctuary for their ground-truth data used in this study. The use of bathymetry processing was assisted by the Slide Rule Earth Platform. No external funding was obtained for this research. The author declares no conflict of interest.

Author Note

Shobha Mourya Dumpati, MSc, FGS, FRGS, holds Master of Science degree in Geographical Information Systems (GIS) from the University of Aberdeen (2023) and is currently Hydrographic Data Processor at Fugro GB LTD, This academic and professional background informed the development of this study. The author used Grammarly and AI-assisted language tools to support clarity, grammar and formatting during manuscript preparation.

References

Belgiu, M., & Drăguţ, L. (2016). Random forest in remote sensing: A review of applications and future directions. ISPRS Journal of Photogrammetry and Remote Sensing, 114, 24-31.

Breiman, L. (2001). Random forests. Machine Learning, 45(1), 5-32.

Costanza, R., et al. (2014). Changes in the global value of ecosystem services. Global Environmental Change, 26, 152-158.

Dekker, A. G., et al. (2011). Intercomparison of shallow water bathymetry, hydro-optics, and benthos mapping techniques. Limnology and Oceanography: Methods, 9(9), 396-425.

Dennison, W. C., et al. (1993). Assessing water quality with submersed aquatic vegetation. BioScience, 43(2), 86-94.

Duarte, C. M. (1991). Seagrass depth limits. Aquatic Botany, 40(4), 363-377.

Gardner, T. A., et al. (2003). Long-term region-wide declines in Caribbean corals. Science, 301(5635), 958-960.

Goodman, J. A., et al. (2013). Coral reef remote sensing: A guide for mapping, monitoring and management. Springer Science & Business Media.

Hedley, J. D., et al. (2005). Simple and robust removal of sun glint for mapping shallow-water benthos. International Journal of Remote Sensing, 26(10), 2107-2112.

Hedley, J. D., et al. (2016). Remote sensing of coral reefs for monitoring and management: A review. Remote Sensing, 8(2), 118.

Hochberg, E. J., et al. (2003). Spectral reflectance of coral reef bottom-types worldwide. Remote Sensing of Environment, 85(2), 159-173.

Hughes, T. P., et al. (2017). Coral reefs in the Anthropocene. Nature, 546(7656), 82-90.

Jackson, J. B., et al. (2014). Status and trends of Caribbean coral reefs. Global Coral Reef Monitoring Network, IUCN.

Kutser, T., et al. (2020). Remote sensing of shallow waters—A 50-year retrospective and future directions. Remote Sensing of Environment, 240, 111619.

Lyons, M. B., et al. (2011). Integrating Quickbird multi-spectral satellite and field data. Remote Sensing, 3(1), 42-64.

Lyzenga, D. R. (1978). Passive remote sensing techniques for mapping water depth and bottom features. Applied Optics, 17(3), 379-383.

Maritorena, S., et al. (1994). Diffuse reflectance of oceanic shallow waters. Limnology and Oceanography, 39(7), 1689-1703.

Mumby, P. J., et al. (1997). Coral reef habitat mapping: How much detail can remote sensing provide? Marine Biology, 130(2), 193-202.

Neumann, T. A., et al. (2019). The Ice, Cloud, and Land Elevation Satellite-2 (ICESat-2): Science requirements, concept, and implementation. Remote Sensing of Environment, 190, 260-273.

Nordlund, L. M., et al. (2016). Seagrass ecosystem services and their variability across genera and geographical regions. PLoS ONE, 11(10), e0163091.

Parrish, C. E., et al. (2019). Validation of ICESat-2 ATLAS bathymetry and analysis of ATLAS's bathymetric mapping performance. Remote Sensing, 11(14), 1634.

Phinn, S. R., et al. (2018). Multi-scale, object-based image analysis for mapping geomorphic and ecological zones on coral reefs. International Journal of Remote Sensing, 33(12), 3768-3797.

Pohl, C., & Van Genderen, J. L. (1998). Multisensor image fusion in remote sensing. International Journal of Remote Sensing, 19(5), 823-854.

Rodriguez-Galiano, V. F., et al. (2012). An assessment of the effectiveness of a random forest classifier for land-cover classification. ISPRS Journal, 67, 93-104.

Roelfsema, C. M., et al. (2018). Coral reef habitat mapping: A combination of object-based image analysis and ecological modelling. Remote Sensing of Environment, 208, 27-41.

Thomas, N., et al. (2021). Space-borne cloud-native satellite-derived bathymetry models using ICESat-2 and Sentinel-2. Geophysical Research Letters, 48(9), e2020GL092170.

Traganos, D., et al. (2018). Estimating satellite-derived bathymetry with Google Earth Engine and Sentinel-2. Remote Sensing, 10(6), 859.

Waycott, M., et al. (2009). Accelerating loss of seagrasses across the globe threatens coastal ecosystems. PNAS, 106(30), 12377-12381.

Wedding, L. M., et al. (2008). Using bathymetric lidar to define nearshore benthic habitat complexity. Remote Sensing of Environment, 112(11), 4159-4165.